Scientia Iranica B (2022) 29(4), 1838–1852

Sharif University of Technology
Scientia Iranica
Transactions B: Mechanical Engineering
http://scientiairanica.sharif.edu

One-day ahead forecasting of energy production from run-of-river hydroelectric power plants with a deep learning approach

M. Bilgili[a], S. Keiyinci[b,*], and F. Ekinci[c]

a. *Department of Mechanical Engineering, Ceyhan Engineering Faculty, Cukurova University, Adana 01950, Turkey.*
b. *Department of Automotive Engineering, Faculty of Engineering, Cukurova University, Adana 01380, Turkey.*
c. *Department of Energy System Engineering, Faculty of Engineering, Adana Alparslan Turkes Science and Technology University, Adana 01250, Turkey.*

Received 1 July 2021; received in revised form 30 October 2021; accepted 7 March 2022

KEYWORDS
Adaptive Neuro-Fuzzy Inference System (ANFIS);
Deep learning;
Energy production;
Long Short-Term Memory (LSTM);
Run-of-river hydroelectric power plant.

Abstract. Accurate energy production forecasting is critical when planning energy for the economic development of a country. A deep learning approach based on Long Short-Term Memory (LSTM) to predict one-day-ahead energy production from the run-of-river hydroelectric power plants in Turkey was introduced in the present study. Furthermore, to compare the prediction accuracy, the methods of Adaptive Neuro-Fuzzy Inference System (ANFIS) with Fuzzy C-Means (FCM), ANFIS with Subtractive Clustering (SC), and ANFIS with Grid Partition (GP) were utilized. The predicted values obtained by the application of these four methods were evaluated with detected values. The correlation coefficient (R), Mean Absolute Error (MAE), Mean Absolute Percentage Error (MAPE), and Root Mean Square Error (RMSE) were used as quality metrics for prediction. The comparison showed that the LSTM neural network provided higher accuracy results in short-term energy production prediction than other ANFIS models used in the study.

© 2022 Sharif University of Technology. All rights reserved.

1. Introduction

Hydroelectric energy is the largest renewable energy source that is substantially critical to more than 160 countries in the world [1–3]. By the end of 2018, 15.9% of global electricity was generated by hydroelectric power, and hydroelectricity also represented more than 62% of electricity generated from renewable sources worldwide. Hydroelectric power generation reached approximately 4,200 TWh, making the highest ever contribution from renewable energy sources. Approximately, 22 GW hydropower capacity was commissioned and the world's total installed power capacity increased to 1,292 GW [4].

Energy plant investments are incredibly high, especially in hydropower plants; besides, the cost and environmental effects should be carefully considered. To be able to decide on sustainable solutions in energy-related decisions, accurate estimation is a crucial subject. Accurate energy production estimation from run-of-river or small hydropower plants is essential in many decision-making areas. Meanwhile, network demand forecasting with a time series problem must also be made to realize that the provided power is fully consumed. Short-term forecasting is crucial to planning a backup power supply, providing the ongoing power supply, and performing energy operations between power stations [5]. The power generation of a small hydroelectric power plant refers to a dynamic

*. *Corresponding author.*
E-mail address: skeiyinci@cu.edu.tr (S. Keiyinci)

doi: 10.24200/sci.2022.58636.5825

process that shows the maximum production capacity under certain hydrological and meteorological conditions. It is also easily affected by climate, hydrology, and installation capacity. Therefore, estimating the power generation of a small hydroelectric system is a complex problem with non-linear and multi-factor dynamics [6].

The possibility of accurately predicting the fundamental trends in the energy production of renewable power plants supplies essential benefits to both the facility management and investors. For energy companies, reasonable estimates of future electricity generation are essential to planning resources to avoid shortcomings and maximize profits in the electricity trade. Policy-makers need to make an appropriate plan for hydroelectric power plant development and achieve this successfully. Policy-makers should constantly track the electricity load in the hydroelectric market and check if the target fits the actual condition. If the hydroelectric energy production is higher than consumer demand, the excess capacity of hydroelectric energy will arise. Conversely, a lower hydroelectric energy production than the demand for hydroelectric consumption will produce a shortage of hydroelectric supply. Also, climate change and natural variability of water flow in rivers where power plants are set up substantially affect the run-of-river hydroelectric power plants [7].

Related literature indicates that the importance of energy production, water inflow, and water level forecasting methods associated to hydropower plants is gradually increasing worldwide. However, forecasting energy production from the run-of-river hydroelectric power plants is not a simple task due to complex factors such as internal faults, scheduled plant closures, power grid faults, floods, extreme weather conditions, water inflow, etc. Since hydroelectric power is a type of electrical energy, run-of-river hydroelectricity consumption is forecasted, similar to the forecasting models for other energy consumption types [7]. The published prediction models are generally classified under four categories: statistical, physical, artificial intelligence, and hybrid models. However, many existing models typically require historical observations or complex independent variables such as atmospheric air temperature, reservoir inflow, and precipitation. Generally, two major categories are valid for classification: the regression model and the time-series approach [8]. The regression model must accurately determine certain descriptive or independent variables that may affect energy production in a plant to estimate the energy production efficiently. On the other hand, in the time series approach, energy production can be modeled as a function of the historical data [9].

Various studies examine energy production, water inflow, and water level forecasting methods related to the hydropower plants in the world. Artificial Neural Network (ANN) [10–15], Artificial Neural Network model with Artificial Bee Colony (ANN-ABC) algorithm [16], Numerical Weather Prediction (NWP) model [17–19], Autoregressive Integrated Moving Average (ARIMA) model [13,20,21], Seasonal Auto-Regressive Iterative Moving Average (SARIMA) model [21], a Model for Assessment of Energy Demand (MAED) [22], Grey Model (GM) [23,24], Correlation Analysis Method (CAM), Complementary Modeling Framework (CMF) [25], least squares Support Vector Regression (SVR) ensemble learning approach, Bayesian regularization with Echo State Network (BESN-ESN) [26], Regression Analysis (RA) [27], Support Vector Machines (SVMs) [28], Genetic Algorithm-Support Vector Machines (GA-SVM) [29], Grey Wolf Optimization method coupled with an Adaptive Neuro-Fuzzy Inference System (GWO-ANFIS) [30] approaches have been widely applied by some researchers for this purpose. Quite good predictive results are obtained, especially in complex non-linear problems and, thus, energy production estimation can be made using artificial intelligence algorithm-based methods. Artificial neural networks have the capabilities to not only learn power generation series but also model an ambiguous non-linear relationship between energy production and its independent variables. Besides, fuzzy logic and machine learning approaches have recently been applied in energy production estimation, and relatively good performances have been obtained. In some academic studies, statistical and probabilistic approaches have been proposed primarily for long-term load estimates.

As can be understood from the literature studies mentioned above, various studies have been carried out in many countries to estimate energy production from hydroelectric power plants. Also, a reasonable estimate for energy consumption helps optimize plant operational planning and control operational management. Energy production in hydroelectric power plants is dynamic; however, a control system can record dynamic time-series data to establish a relationship between current and historical working conditions.

This study predicts energy production from run-of-river hydroelectric power plants with a time series approach. This is a time series problem since the current energy production from run-of-river hydroelectric power plants is directly related to previous operating conditions or data. As is known, the time series estimation technique is regression analysis. Traditional models usually cannot learn time series data as they cannot store previous information, leading to a limited ability to estimate long-term time-series data, e.g., energy production. Thus, a new method with the ability to process significant amounts of high-quality data is needed. Hence, the present study adopted

a Long Short-Term Memory (LSTM) neural network that dynamically recalls historical information to estimate energy production from run-of-river hydroelectric power plants. Studies in which deep learning approaches based on the LSTM network are successfully applied are included in the literature. Refs. [31–42] can be examined for detailed information.

Within the scope of this study, the following subjects are at focus:

- A deep learning approach based on LSTM is presented to predict energy production from run-of-river hydroelectric power plants in Turkey. Studies on the deep learning-based LSTM neural network to predict electricity generation from river-type hydroelectric power plants are limited in the literature;
- As for forecast models published in the literature on hydropower, many studies have been carried out with the aim of predicting sizeable hydroelectric power plants and they have focused mainly on estimating river flows such as streamflow, reservoir inflow, precipitation, and runoff. However, the number of studies on estimating small hydropower generation is limited, especially in Turkey. In this paper, LSTM, a helpful attempt at deep learning, is applied to study energy production from Turkey's run-of-river hydroelectric power plants;
- Additionally, within the scope of the research, the findings acquired from the LSTM method were correlated with those of the ANFIS models using the same data to prove the performance of the current approach used in the study and the differences between them were interpreted.

2. Material and methods

2.1. Adaptive neuro-fuzzy inference system

Adaptive Network Fuzzy Inference System (ANFIS) is a universal estimator. It can be used for any proper continuous function in a compact setup to any degree of accuracy. ANFIS is expressed as a network statement of Sugeno-type fuzzy systems equipped with neural learning capabilities and creates fuzzy if-then rules with appropriate Membership Functions (MF) from input-output by employing a neural network learning algorithm. FIS development procedure using the ANN framework is stated ANFIS [43,44]. In the working principle of an ANFIS model, the system is first trained similarly to ANN. After that, the system is conducted as a fuzzy inference system. In this sense, ANFIS's integration of both ANN and FIS principles has led to integration of the advantages of both systems into a single system [45].

The neuro-fuzzy model contains a total of five layers as a multi-layered neural-network-based fuzzy system. The network structure contains input and output nodes representing input states and output response, respectively, and nodes in hidden layers acting as Membership Functions (MFs) and rules. Thus, the disadvantage of an observer's difficulty in understanding or replacing a standard feedforward multi-layered network is avoided [46,47]. Figure 1 shows type-3 fuzzy reasoning and corresponding equivalent ANFIS architecture (Type-3 ANFIS), respectively. In the structure, a circle represents a fixed node, while a square represents an adaptive node. Two inputs, x and y, and one output, f, are considered, as it is a

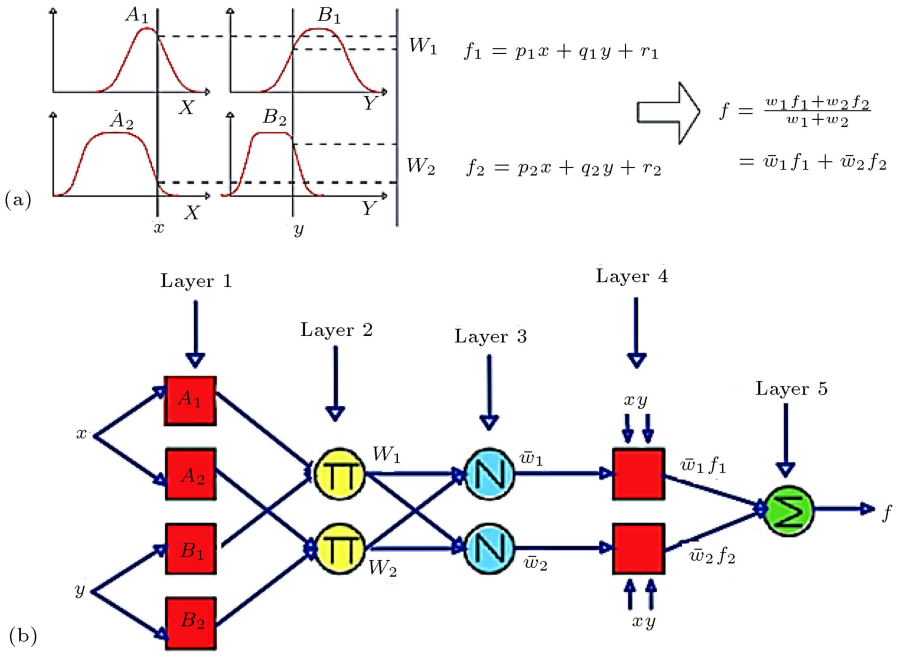

Figure 1. (a) Type-3 fuzzy reasoning. (b) Equivalent ANFIS (Type-3 ANFIS) [44].

simple structure. Thanks to its high interpretability, computational efficiency, and built-in optimal and adaptable techniques, the Sugeno model is the most widely applied fuzzy model found in the relevant literature.

2.2. Long Short-Term Memory (LSTM) neural network

LSTM is a repetitive neural network designed by Hochreiter and Schmidhuber [48]. The architecture allows LSTM networks to either carry information for the long term or forget the information. This process is controlled by gates that are some kind of activation function in this case. The decision of whether the information will be passed along or not falls on the activation function. LSTMs that eliminate the long-term dependencies of RNN are specific types of RNN, thus learning long-term dependencies and remembering data for a long time by default. They are used in processing, prediction, and classification of information based on time series data. Their use in speech recognition, machine translation, language modeling for tourism, and stock prediction has yielded successful results. Studies on LSTM have shown their successful applications including their possible application to energy forecasting.

LSTM networks address the issue of retaining information for the long term. Standard recurrent neural networks rely on a simple tan-hyperbolic layer. LSTM network has the same structure, but it also has additional layers that interact in a particular manner. Figure 2 shows the architecture of a typical LSTM block. This architecture gives LSTM networks the ability to carry information for the long term or forget it. This process is controlled by gates that are some kind of activation function in this case. The decision of whether the information will be passed along or not falls on the activation function. The chain structure of LTSM comprises four neural networks and different memory blocks, namely cells. The cells retain information and the gates manipulate memory. LTSM networks address the issue of retaining information for the long term. Standard recurrent neural networks rely on a simple tan-hyperbolic layer. LTSM network has the same structure, but also has additional layers that interact in a particular manner. An LSTM unit comprises a cell, an input gate, an output gate, and a forget gate. The forget gate was not initially included and was later proposed by Gers et al. [49] to allow a network to reset its state. LSTM architecture comprises a group of regularly reconnected sub-networks, i.e., memory blocks. The memory block maintains its state as time passes and regulates information flow through non-linear gating units. Input activation flow into the memory cell is controlled by the input gate. The output gate controls cell activations' output flow into the remaining network. Finally, the forget gate was included in the memory block.

2.2.1. Forget gate

Forget gate (Figure 3) removes the now-redundant information in the cell state. The gate is fed with two inputs $x^{(t)}$ (input at a particular time) and $y^{(t-1)}$ (previous cell output), which are then multiplied by weight matrices and added to the bias term. An activation function processes the resultant, yielding a binary output. For a particular cell state, the information is forgotten if the output is zero; it is retained for future use if the output is 1.

$$f^{(t)} = \sigma\left(W_f x^{(t)} + R_f y^{(t-1)} + p_f \odot c^{(t-1)} + b_f\right), \qquad (1)$$

where W_f, R_f, and p_f are the weights associated with $x^{(t)}$, $y^{(t-1)}$, and $c^{(t-1)}$ respectively, while b_f is for the bias weight vector.

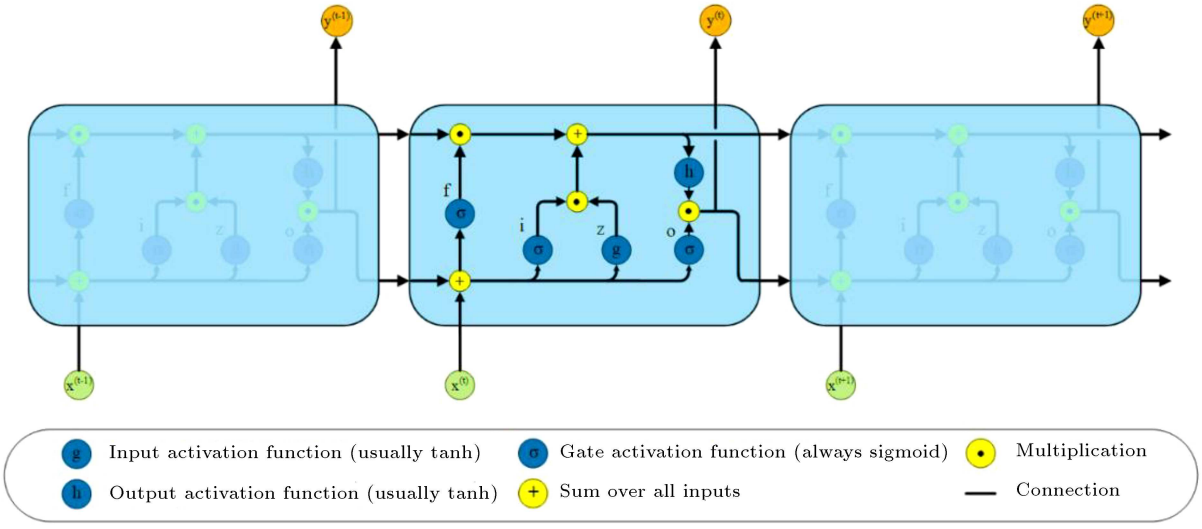

Figure 2. The architecture of a typical LSTM block.

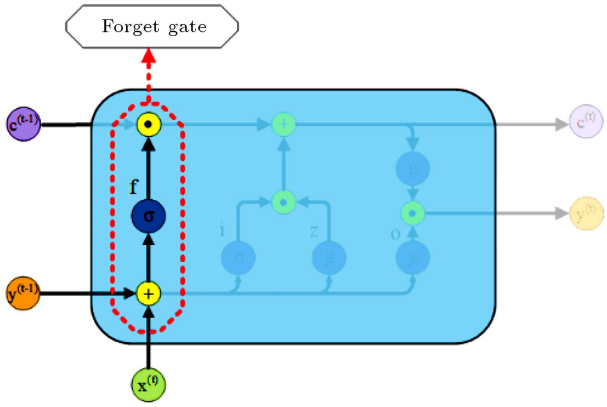

Figure 3. Forget gate in the LSTM memory block.

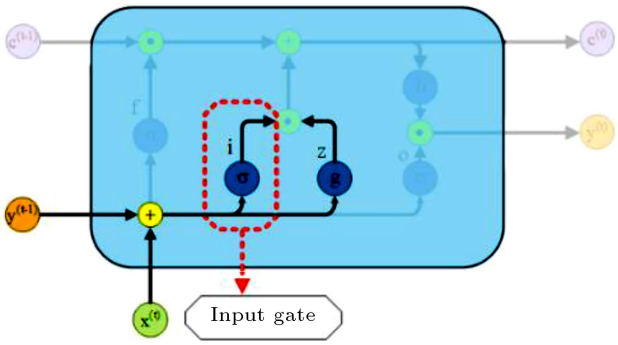

Figure 4. Input gate in the LSTM memory block.

2.2.2. Input gate

The input gate (Figure 4) adds helpful information to the cell state. The sigmoid function firstly regulates the information and similarly filters the values to that of forget gate with inputs $y^{(t-1)}$ and $x^{(t)}$. The $\tan h$ function, which yields an output of values ranging from -1 to $+1$, is used to create a vector containing all the possible values from $y^{(t-1)}$ and $x^{(t)}$. Finally, the vector values and regulated values are multiplied to obtain helpful information.

$$i^{(t)} = \sigma\left(W_i x^{(t)} + R_i y^{(t-1)} + p_i \odot c^{(t-1)} + b_i\right), \quad (2)$$

$$z^{(t)} = g\left(W_z x^{(t)} + R_z y^{(t-1)} + b_z\right), \quad (3)$$

where:

$\odot$	Point-wise multiplication of two vectors
W_i, W_z	Weights associated with $x^{(t)}$
R_i, R_z	Weights associated with $y^{(t-1)}$
p_i	Weight associated with $c^{(t-1)}$
b_i	Bias vector
b_z	Bias weight vector

2.2.3. Output gate

The output gate (Figure 5) extracts helpful information from the current cell state and presents it as an output.

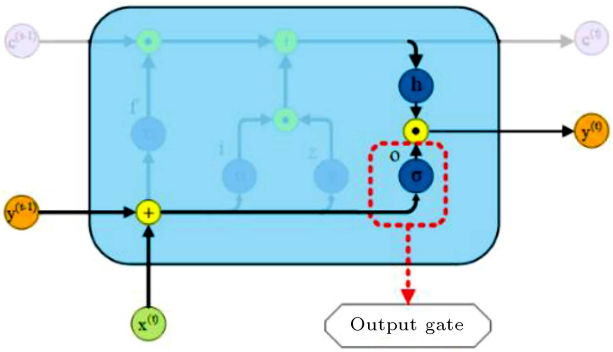

Figure 5. Output gate in the LSTM memory block.

The application of the $\tan h$ function to the cell firstly generates a vector. The sigmoid function regulates the information and filters the values that will be remembered using inputs $y^{(t-1)}$ and $x^{(t)}$. Finally, the vector and regulated values are multiplied as outputs and inputs to the next cell. The output of the block is regularly reconnected to the block input and all gates.

$$o^{(t)} = \sigma\left(W_o x^{(t)} + R_o y^{(t-1)} + p_o \odot c^{(t-1)} + b_o\right), \quad (4)$$

where W_o, R_o, and p_o are the weights associated with $x^{(t)}$, $y^{(t-1)}$, and $c^{(t-1)}$, respectively, while b_o is the bias weight vector.

Finally, the block output combining the current cell value $c^{(t)}$ with the current output gate value is calculated through the following equation:

$$y^{(t)} = g\left(c^{(t)}\right) \odot o^{(t)}, \quad (5)$$

where σ, g, and h in the above steps represent point-wise non-linear activation functions.

$$\sigma(x) = \frac{1}{1+e^{1-x}} \qquad \text{(logistic sigmoid)}.$$

The logistic sigmoid is the gate activation function and the hyperbolic tangent $g(x) = h(x) = \tan h(x)$ is often the block input and output activation function [50].

2.3. Error analysis

In our study, four statistical error criteria including Mean Absolute Error (MAE), Root Mean Square Error (RMSE), Mean Absolute Percentage Error (MAPE), and correlation coefficient (R) are used for assessing the goodness of a model to estimate an observed output variable. Their calculation methods are given as follows [51–53]:

Mean absolute error:

$$MAE = \frac{1}{N}\sum_{i=1}^{N} |p(i) - o(i)|. \quad (6)$$

Root mean square error:

$$RMSE = \sqrt{\frac{1}{N}\sum_{i=1}^{N}[p(i) - o(i)]^2}. \quad (7)$$

Mean absolute percentage error:

$$MAPE = \frac{1}{N}\sum_{i=1}^{N}\frac{|p(i) - o(i)|}{o(i)} \times 100. \quad (8)$$

The correlation coefficient:

$$R = \left(\sum_{i=1}^{N}[p(i) - \bar{p}]\,[o(i) - \bar{o}]\right) \Bigg/ \left(\sqrt{\sum_{i=1}^{N}[p(i) - \bar{p}]^2}\sqrt{\sum_{i=1}^{N}[o(i) - \bar{o}]^2}\right), \quad (9)$$

where $p(i)$ and $o(i)$ are the predicted and observed values at time i, respectively; $\bar{p}$ and $\bar{o}$ are the means of the predicted and actual values, respectively, and the total number of data is represented by N.

3. Results and discussion

3.1. Data analysis and model structure

Since topographical conditions make small power plant development more convenient in Turkey, run-of-river hydroelectric power plants have shown significant development in recent years. As of the end of 2020, the total installed power value of these power plants was approximately 8 GW. This is equivalent to 8.4% of Turkey's total installed power capacity. Therefore, forecasting studies over energy production from the run-of-river hydroelectric power plants have become very important, especially for Turkey. Moreover, since Turkey is mainly dependent on foreign sources of electricity generation, accurate and precise forecasting of energy production is very important. Therefore, this study aims to predict short-term energy generation from the run-of-river hydroelectric power plants for Turkey. The data used for this objective in this study cover daily energy production from run-of-river hydroelectric power plants in Turkey. These data were obtained by the Turkish Electricity Transmission Corporation (TETC) by collecting an energy generation of 576 run-of-river power plants in 25 river basins of Turkey. The location of Turkey's 25 river basins is presented in Figure 6.

In this study, a time-series analysis-based LSTM neural network was proposed and applied to predict the energy production of run-of-river hydroelectric power plants in Turkey. In the LSTM neural network simulation, the measurement inputs were divided into two datasets. The first one, the training dataset, was employed for the model's training, while the second one, the testing dataset, was employed for over-fitting model validation. The evaluation criteria comprised RMSE, MAPE, MAE, and R. In addition to the LSTM neural network, three different approaches including ANFIS-FCM, ANFIS-SC, and ANFIS-GP were used. Then, the ANFIS models were analyzed. The results

Figure 6. Location of Turkey's 25 river basins.

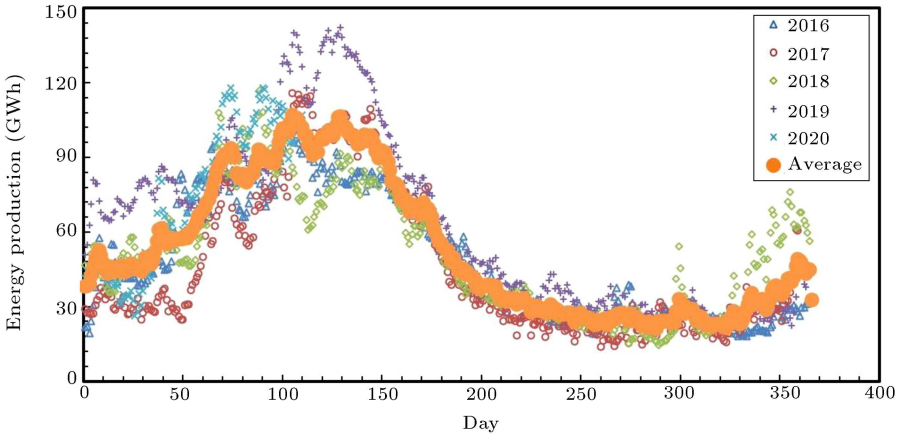

Figure 7. Energy production from the run-of-river hydroelectric power plants in Turkey.

were compared using performance statistics. The number of MFs varied between 2 and 10, and the number of iterations varied between 50 and 300.

Figure 7 shows the energy production data used in the present work. They were obtained from the TETC in Turkey as a daily dataset from January 01, 2016 to April 19, 2020 [54]. Turkey's daily energy production from the run-of-river hydroelectric power plants ranged from 13.87 GWh to 142.11 GWh between January 01, 2016 and April 19, 2020. The minimum daily energy production was realized on September 17, 2017, while the maximum daily energy production was on May 09, 2019. During these five years, the average daily energy production was calculated to be approximately 54 GWh. A total of 1571 samples were partitioned into two sections as the first 80% section was the train set and the last 20% section was the test.

The water carried by the rivers may vary in amount every year or every season of the year. Some rivers may dry out entirely in some arid years, or rivers may overflow by not fitting in their beds in some rainy years. Similarly, different amounts of water streams may increase in different seasons of the year. Given that energy production is a dynamic process depending on river water flow and many independent variables, energy production throughout the year exhibits a significant change daily and monthly. As shown in Figure 7, energy production increases upon increasing the amount of water flow in river water due to excessive rainfall, especially in March, April, and May. Although energy production in hydroelectric power plants is dynamic, a control system can record dynamic data to establish a time-series relationship between current and historical working conditions. This study predicts the energy production from the run-of-river hydroelectric power plants using a time series approach. The proposed method processes the previous load series data instead of various factors such as time, water stream, climate, and socio-economic activities that affect energy production because it is not always easy to obtain and measure these independent variables.

3.2. Results of the LSTM network

Table 1 gives the prediction performances for the LSTM neural network with different accuracy criteria. The values shown in bold indicate the best results

Table 1. The prediction performances for the LSTM neural network models.

Model	Number of hidden layers	MAE (GWh)	MAPE (%)	RMSE (GWh)	R
LSTM-1	**5**	**2.71**	**5.98**	**3.62**	**0.9914**
LSTM-2	10	2.73	6.03	3.62	0.9914
LSTM-3	15	2.74	6.04	3.62	0.9914
LSTM-4	20	2.76	6.07	3.63	0.9914
LSTM-5	25	2.78	6.12	3.65	0.9913
LSTM-6	30	2.77	6.12	3.66	0.9913
LSTM-7	50	2.79	6.12	3.63	0.9914
LSTM-8	75	2.77	6.10	3.64	0.9914
LSTM-9	100	2.80	6.15	3.66	0.9913
LSTM-10	125	2.77	6.06	3.65	0.9913
LSTM-11	150	2.81	6.17	3.65	0.9913
LSTM-12	175	2.84	6.16	3.72	0.9910
LSTM-13	200	2.81	6.15	3.68	0.9911

Table 2. The prediction performances for the ANFIS-FCM models.

Model	Number of MFs	MAE (GWh)	MAPE (%)	RMSE (GWh)	*R*
ANFIS-FCM-1	2	2.82	6.23	3.72	0.9910
ANFIS-FCM-2	3	2.82	6.20	3.72	0.9909
ANFIS-FCM-3	4	2.80	6.16	3.66	0.9912
ANFIS-FCM-4	**5**	**2.79**	**6.14**	**3.67**	**0.9912**
ANFIS-FCM-5	6	2.82	6.15	3.69	0.9911
ANFIS-FCM-6	7	2.88	6.31	3.77	0.9907
ANFIS-FCM-7	8	2.86	6.27	3.75	0.9908
ANFIS-FCM-8	9	2.84	6.22	3.74	0.9909
ANFIS-FCM-9	10	2.87	6.28	3.79	0.9906

in all tables. The evaluation criteria in this table were considered according to the forecasting values obtained from the test process results. A total of 13 LSTM neural network models ranging from 5 to 200 hidden layers were tried and tested. According to this table, the performance values obtained using different hidden layer numbers are quite close to each other. For example, MAPE values for all the models were calculated to be between 5.98% and 6.17%, while R values were obtained to be between 0.9910 and 0.9914. However, the best result was observed when the number of the hidden layers was equal to 5 with the values of 2.71 GWh MAE, 5.98% MAPE, 3.62 GWh RMSE, and 0.9914 R. The results demonstrated that the LSTM models performed satisfactorily in forecasting daily energy production.

Observed and predicted daily energy production data for the LSTM network are shown in Figure 8(a). The daily production variations could be observed in the energy production time series. As seen from Figure 8, the prediction of the energy production time series is quite consistent with the actual values in the testing. The testing values were presented in Figure 8(b) in more detail. In addition to Figure 8(a) and (b), Figure 8(c) shows the regression plots of actual and predicted values of the energy production data from the LSTM neural network. This figure shows that good estimation results are obtained due to the formation of data pairs closer to the 45° line.

3.3. Results of the ANFIS-FCM model

Table 2 shows different evaluation criteria values for the ANFIS-FCM model. A total of 9 ANFIS-FCM models ranging from 2 to 10 MFs were tried and tested. In terms of a general evaluation, it was observed that the performance values obtained from all ANFIS-FCM models gave very close results to each other. However, a small number of the MFs did not yield satisfactory results due to the non-good partitioning of the inputs. In addition, a large number of MFs did not give good results, as this led to the use of a large number of nodes and fuzzy rules that add to the computation

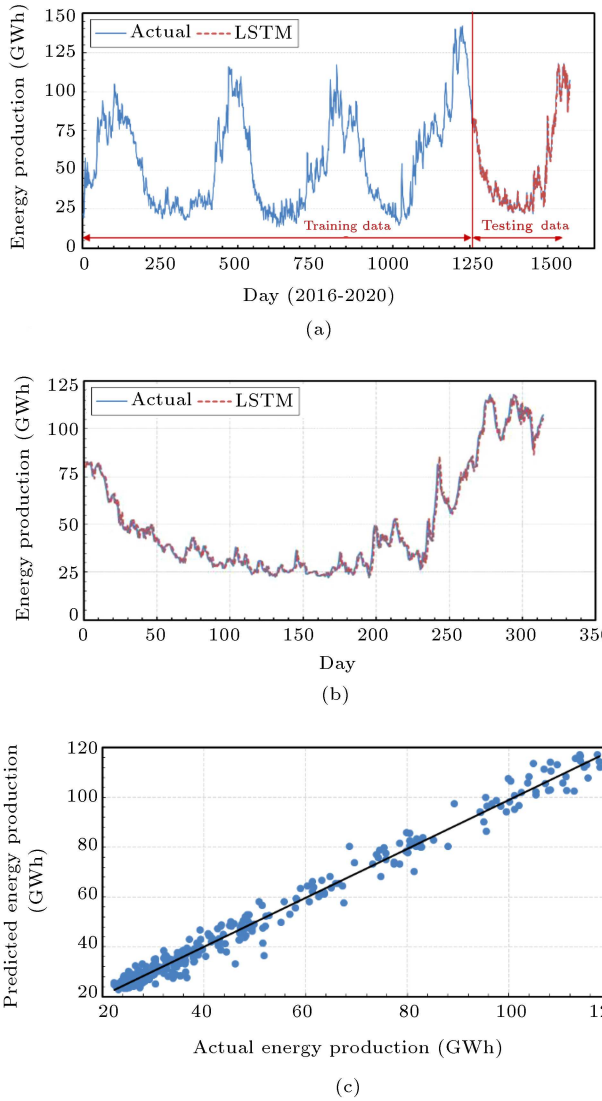

Figure 8. (a) The daily time series energy production data with actual values (blue) and predicted values (red) for the LSTM neural network model. (b) Actual values (blue) and predicted values (red) of the testing of the energy production data for the LSTM neural network model. (c) Regression plots of the actual values and predicted values of the energy production data for LSTM neural network model.

time. According to the test process results, the best performance was obtained from MFs = 5 with 2.79 GWh MAE, 6.14% MAPE, 3.67 GWh RMSE, and 0.9912 R.

The daily time series energy production data with actual and predicted values for the ANFIS-FCM method are presented in Figure 9(a). As revealed in Figure 9, the energy production time series estimates agree with the actual values in the test part. Figure 9(b) shows the test values so as to take a closer look at prediction results. In addition to Figure 9(a) and (b), Figure 9(c) shows the regression plots of the actual and predicted values of the energy production data from the ANFIS-FCM method. This graph presents the distribution of actual and predicted values and shows how consistent the model results are with the actual data. A strong linear relationship between actual and predicted values in this figure shows that the ANFIS-FCM method predicts daily energy production from run-of-river hydroelectric power plants with remarkable accuracy (99%).

3.4. Results of the ANFIS-SC model

Similarly, the prediction methodology was applied to the ANFIS-SC model. Different cluster radius sets were analyzed in the range of 0.1 to 0.9. Table 3 gives the results obtained from the testing process. According to the table, all models of ANFIS-SC have given accuracy values very close to each other. However, the ANFIS-SC-4 and 5 models gave better RMSE and R estimates. The MAE, MAPE, RMSE, and R values were obtained for these models as 2.81 GWh, 6.16%, 3.70 GWh, and 0.9911, respectively. Results showed that low values of the cluster radius did not allow good mapping of the ANFIS-SC model. However, the high values of the cluster radius made the training more difficult and led to overfitting or memorization of undesirable inputs.

The actual and predicted daily energy production data are shown in Figure 10(a) for the ANFIS-SC method. Figure 10(b) shows the testing values for the last 20% of the dataset. Figure 10(c) shows the

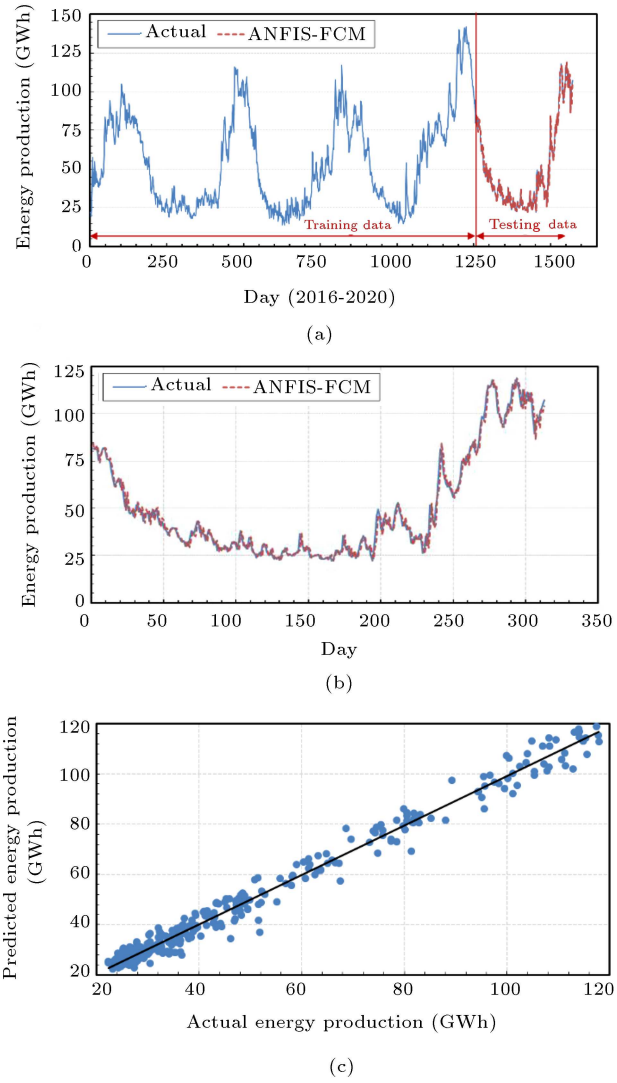

Figure 9. (a) The daily time series energy production data with actual values (blue) and predicted values (red) for the ANFIS-FCM method. (b) Actual values (blue) and predicted values (red) of the testing of energy production data for the ANFIS-FCM method. (c) Regression plots of the actual values and predicted values of the energy production data for ANFIS-FCM method.

Table 3. The prediction performances for the ANFIS-SC models.

Model	Radius of the cluster	MAE (GWh)	MAPE (%)	RMSE (GWh)	R
ANFIS-SC-1	0.1	2.84	6.25	3.74	0.9909
ANFIS-SC-2	0.2	2.85	6.28	3.75	0.9908
ANFIS-SC-3	0.3	2.82	6.16	3.72	0.9909
ANFIS-SC-4	**0.4**	**2.81**	**6.16**	**3.70**	**0.9911**
ANFIS-SC-5	**0.5**	**2.81**	**6.16**	**3.70**	**0.9911**
ANFIS-SC-6	0.6	2.81	6.18	3.70	0.9910
ANFIS-SC-7	0.7	2.81	6.18	3.71	0.9910
ANFIS-SC-8	0.8	2.81	6.20	3.71	0.9910
ANFIS-SC-9	0.9	2.81	6.19	3.71	0.9910

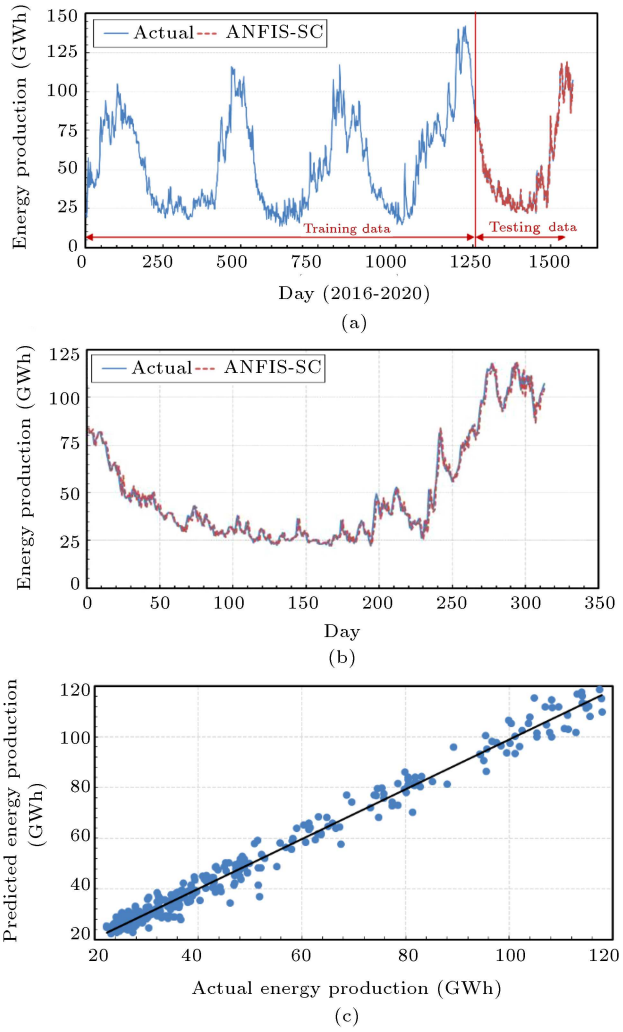

Figure 10. (a) The daily time series energy production data with actual values (blue) and predicted values (red) for the ANFIS-SC method. (b) Actual values (blue) and predicted values (red) of the testing of the energy. (c) Regression plots of the actual values and predicted values of the energy production data for ANFIS-SC method.

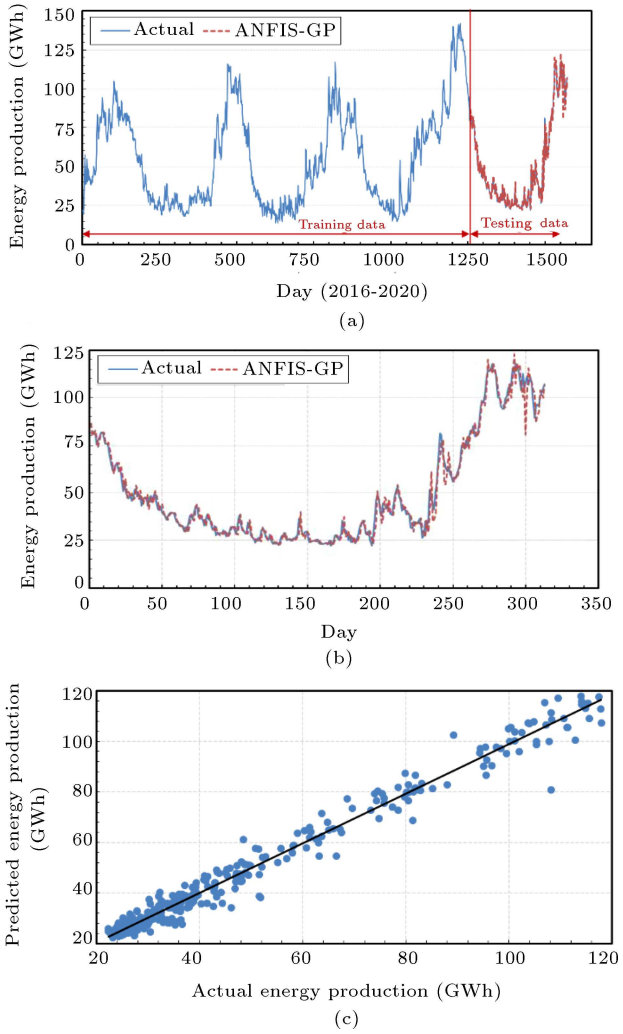

Figure 11. (a) The daily time series energy production data with actual values (blue) and predicted values (red) for the ANFIS-GP method. (b) Actual values (blue), and predicted values (red) of the testing of the energy production data for the ANFIS-GP method. (c) Regression plots of the actual values and predicted values of the energy production data for ANFIS-GP method.

regression plots of the actual predicted values of the energy production. The R-value was calculated to be 0.9911 for the ANFIS-SC method.

3.5. Results of the ANFIS-GP model

Similarly, the prediction methodology was applied to the ANFIS-GP model. This model used the Gaussian membership function and linear membership function as the input and output, respectively. The number of MFs received was 2 and 3. Table 4 gives the results obtained from the testing process. With a review of the table, it is understood that the model obtained using the ANFIS-GP approach predicts the energy production from run-of-river hydroelectric power plants with an accuracy rate of 98.81% according to the performance evaluation criterion, R. The daily time series energy production data with actual and predicted values for the ANFIS-GP method are presented in Figure 11(a). As seen in the figure, all ANFIS-SC

Table 4. The prediction performances for the ANFIS-GP models. Best results are shown in bold.

Model	Number of MFs	MAE (GWh)	MAPE (%)	RMSE (GWh)	R
ANFIS-GP-1	**2**	**2.99**	**6.40**	**4.26**	**0.9881**
ANFIS-GP-2	3	6.21	10.44	16.18	0.8574

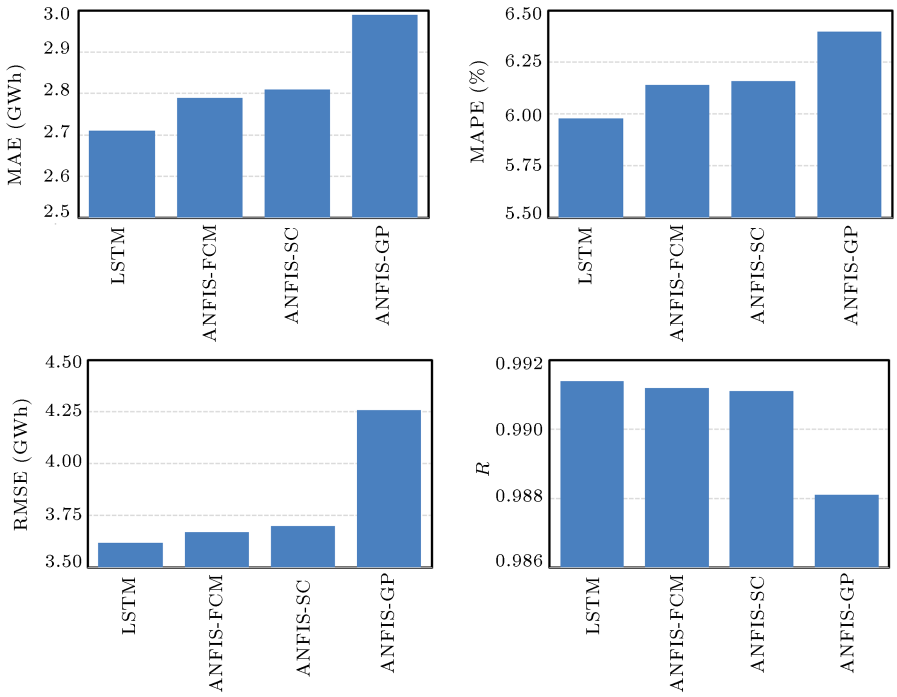

Figure 12. Comparison of the models.

models have produced almost similar results in terms of accuracy measures. Figure 11(b) and (c) show a close look at test data and the regression plots of the dataset, respectively. For this model, the MAE, MAPE, RMSE, and R values were calculated as 2.99 GWh, 6.40%, 4.26 GWh, and 0.9881, respectively.

3.6. Comparison of the models

LSTM neural network is one of the approaches that enjoys good prediction performance among deep learning methods. Therefore, this study compares the prediction performances of machine learning algorithms including ANFIS-FCM, ANFIS-SC, and ANFIS-GP with the performance of the deep learning method. The LSTM model can decide on the relationships between features while optimizing their network. Thanks to its memory structure, features can be forgotten or remembered. On the other hand, ANFIS is one of the most important machine learning approaches that combines the advantages of both neural and fuzzy systems in a single model. Besides, having a very high learning speed, the ANFIS algorithm provides high accuracy in the testing phase. In addition, it is easy to perform and can be used to predict different application areas. In Figure 12, the best evaluation criteria resulting from all the models used in the study were represented. As revealed by the table, the LSTM neural network model yielded the best result with the values of 2.71 GWh MAE, 5.98% MAPE, 3.62 GWh RMSE, and 0.9914 R. The ANFIS-FCM and ANFIS-SC models showed relatively similar results in terms of accuracy measures. However, the ANFIS-FCM model resulted in slightly better MAE, MAPE, RMSE, and R. For this model, the MAE, MAPE, RMSE, and R values were calculated as 2.79 GWh, 6.14%, 3.62 GWh, and 0.9912, respectively. Figure 12 shows that the ANFIS-GP model yielded less accurate results in comparison with other models. In summation, the results of the statistical indexes are shown in Figure 12; accordingly, the LSTM neural network achieved more good accuracy than the other models.

In Table 5, typical studies on energy production and water flow estimation methods related to hydroelectric power plants and the results within the scope of this study are presented for comparison purposes. In related studies, it is seen that the R value varies between 0.7239 and 0.9999. However, the R value achieved in this study was 0.9914, which was found to be very close to those found by similar studies in the literature.

4. Conclusion

Short-term estimations of daily hydroelectric production for the day ahead are essential for power system representatives to program system operations and decision-making on the electricity market considering the hydroelectric power generation in real electric power plants and electricity market environments. A prediction of energy production that provided data on how much energy can be effectively generated by a particular energy plant in a given period can

Table 5. Some of the typical studies on energy production and water flow forecasting methods related to the hydropower plants in the world.

Ref.	Method	Prediction	Study area	Data time	Data term	Performance criteria
[6]	CAM	Energy production	China	November, 2012 - July, 2015	Monthly	$R = 0.9400$
[12]	ANN	Energy production	Nigeria	1970-2011 and 1984-2011	Monthly	$R = 0.8900$
[14]	ANN	Energy production	Turkey	35-year-long recorded data	Monthly	$R^2 = 0.9820$
[15]	ANN	Energy production	Iraq	2005-2015	Daily	$R = 0.9600$
[20]	ARIMA	Energy production	Ecuador	2000-2015	Monthly	$R = 0.7239$
[23]	GM	Energy production	China	2012-2015	Monthly	$R^2 = 0.9730$
[55]	DNN	Energy production	Turkey	April-September of 2019	Hourly	$R^2 = 0.9999$
[56]	LSTM	Water flow	Brazil	January, 2016-September, 2019	Daily	$R^2 = 0.8519$
[57]	HYPE and ANN	Energy production	Slovenia	January, 2010-December, 2017	Daily	$R^2 = 0.7400$
[58]	ANN-DCSA	Energy production	China	1990-2020	Yearly	$R^2 = 0.8827$
This study	LSTM	Energy production	Turkey	January, 2016-April, 2020	Daily	$R = 0.9914$

become advantageous for optimizing renewable energy marketing. In this study, an LSTM neural network was applied to develop a short-term forecasting model that could forecast daily energy production from Turkey's run-of-river hydroelectric power plants. Forecasting consists of predicting the future situation according to previous or past values. Comparison of the results obtained using the LSTM neural network with those obtained by the traditional ANFIS model showed that LSTM neural network model had a better performance than the ANFIS model under the same model structure and parameters. For example, the LSTM neural network model yielded the best result with 2.71 GWh MAE, 5.98% MAPE, 3.62 GWh RMSE, and 0.9914 R. In addition, the results demonstrated the higher predictive accuracy of the proposed LSTM neural network model and that the model enjoyed a more robust generalization capability, a faster response speed, and greater competitive power in modeling energy production.

The time series method based on the LSTM neural network proposed in this study performed modeling by considering the hidden periodicities in the data. The most crucial advantage of univariate modeling is

that there is no need to obtain independent variables. Consequently, if the energy data contained a periodic fluctuation, an LSTM model based on time series and deep learning could be considered to calculate prediction values. For the future work, different deep learning architectures and functions will be used with hybrid models to improve the accuracy and precision of prediction results.

Acknowledgments

The authors would like to thank the Cukurova University Scientific Research Project Coordination (FBA-2019-11937) for financial support.

Nomenclature

ANFIS	Adaptive Neuro-Fuzzy Inference System
FCM	Fuzzy c-Means
GP	Grid Partition
LSTM	Long Short-Term Memory
MAE	Mean Absolute Error
MAPE	Mean Absolute Percentage Error
R	Correlation coefficient
RMSE	Root Mean Square Error
SC	Subtractive Clustering
b_i	Bias vector
b_z	Bias weight vector
$c^{(t)}$	Current cell value
f	Output
g	Nonlinear activation function
g	Nonlinear activation function
$o(i)$	Observed value
$p(i)$	Predicted value
p_i	Weight associated with $c^{(t-1)}$
R_i, R_z	Weight associated with $y^{(t-1)}$
x	Input
$x^{(t)}$	Input at a particular time
$y^{(t)}$	Block output
$y^{(t-1)}$	Previous cell output
w	Weight
W_i, W_z	Weight associated with x^t
σ	Nonlinear activation function
$\odot$	Point-wise multiplication of two vectors

References

1. Stenberg, V., Rydén, M., Mattisson, T., et al. "Exploring novel hydrogen production processes by integration of steam methane reforming with chemical-looping combustion (CLC-SMR) and oxygen carrier aided combustion (OCAC-SMR)", *Int. J. Greenh. Gas Control*, **74** (May), pp. 28–39 (2018).
2. Chang, X.L., Liu, X., and Zhou, W. "Hydropower in China at present and its further development", *Energy*, **35**(11), pp. 4400–4406 (2010).
3. Yüksek, ö. "Reevaluation of Turkey's hydropower potential and electric energy demand", *Energy Policy*, **36**(9), pp. 3374–3382 (2008).
4. REN21. https://www.ren21.net/. accessed November 30, 2020.
5. Dmitrieva, K. *Forecasting of a Hydropower Plant Energy Production*, Ostfold University College, MSc Thesis (2015).
6. Li, G., Liu, C.X., Liao, S.L., et al. "Applying a correlation analysis method to long-term forecasting of power production at small hydropower plants", *Water (Switzerland)*, **7**(9), pp. 4806–4820 (2015).
7. Wang, S., Yu, L., Tang, L., et al. "A novel seasonal decomposition based least squares support vector regression ensemble learning approach for hydropower consumption forecasting in China", *Energy*, **36**(11), pp. 6542–6554 (2011).
8. Ardakani, F.J. and Ardehali, M.M. "Long-term electrical energy consumption forecasting for developing and developed economies based on different optimized models and historical data types", *Energy*, **65**, pp. 452–461 (2014).
9. Günay, M.E. "Forecasting annual gross electricity demand by artificial neural networks using predicted values of socio-economic indicators and climatic conditions: Case of Turkey", *Energy Policy*, **90**, pp. 92–101 (2016).
10. Stokelj, T., Paravan, D., and Golob, R. "Enhanced artificial neural network inflow forecasting algorithm for run-of-river hydropower plants", *J. Water Resour. Plan. Manag.*, 128(6), pp. 415–423 (2002).
11. Campolo, M., Soldati, A., and Andreussi, P. "Forecasting river flow rate during low-flow periods using neural networks", *Water Resour. Res.*, **35**(11), pp. 3547–3552 (1999).
12. Abdulkadir, T., Salami, A., Anwar, A., et al. "Modelling of hydropower reservoir variables for energy generation: Neural network approach", *Ethiop. J. Environ. Stud. Manag.*, **6**(3), pp. 310–316 (2013).
13. Igboanugo, A.C. "Predicting water levels at Kainji dam using artificial neural networks", *Niger. J. Technol.*, **32**(1), pp. 129–136 (2013).
14. Cobaner, M., Haktanir, T., and Kisi, O. "Prediction of hydropower energy using ANN for the feasibility of hydropower plant installation to an existing irrigation dam", *Water Resour. Manag.*, **22**(6), pp. 757–774 (2008).
15. Hammid, A.T., Sulaiman, M.H.B., and Abdalla, A.N. "Prediction of small hydropower plant power production in Himreen Lake dam (HLD) using artificial neural

network", *Alexandria Eng. J.*, **57**(1), pp. 211–221 (2018).

16. Uzlu, E., Akpinar, A., Özturk, H.T., et al. "Estimates of hydroelectric generation using neural networks with the artificial bee colony algorithm for Turkey", *Energy*, **69**, pp. 638–647 (2014).
17. Monteiro, C., Ramirez-Rosado, I.J., and Fernandez-Jimenez, L.A. "Short-term forecasting model for electric power production of small-hydro power plants", *Renew. Energy*, **50**, pp. 387–394 (2013).
18. Monteiro, C., Ramirez-Rosado, I.J., and Fernandez-Jimenez, L.A. "Short-term forecasting model for aggregated regional hydropower generation", *Energy Convers. Manag.*, **88**, pp. 231–238 (2014).
19. Ahmad, S.K. and Hossain, F. "Maximizing energy production from hydropower dams using short-term weather forecasts", *Renew. Energy*, **146**, pp. 1560–1577 (2020).
20. Mite-León, M. and Barzola-Monteses, J. "Statistical model for the forecast of hydropower production in Ecuador", Int. *J. Renew. Energy Res.*, **8**(2), pp. 1130–1137 (2018).
21. Ediger, V.Ş. and Akar, S. "ARIMA forecasting of primary energy demand by fuel in Turkey", *Energy Policy*, **35**(3), pp. 1701–1708 (2007).
22. Yuksek, O., Komurcu, M.I., Yuksel, I., et al. "The role of hydropower in meeting Turkey's electric energy demand", *Energy Policy*, **34**(17), pp. 3093–3103 (2006).
23. Cheng, C.T., Miao, S.M., Luo, B., et al. "Forecasting monthly energy production of small hydropower plants in ungauged basins using grey model and improved seasonal index", *J. Hydroinformatics*, **19**(6), pp. 993–1008 (2017).
24. Wang, Z.X., Li, Q., and Pei, L.L. "Grey forecasting method of quarterly hydropower production in China based on a data grouping approach", *Appl. Math. Model.*, **51**, pp. 302–316 (2017).
25. Gragne, A.S., Sharma, A., Mehrotra, R., et al. "Improving real-time inflow forecasting into hydropower reservoirs through a complementary modelling framework", *Hydrol. Earth Syst. Sci.*, **19**(8), pp. 3695–3714 (2015).
26. Li, G., Li, B.J., Yu, X.G., et al. "Echo state network with Bayesian regularization for forecasting short-term power production of small hydropower plants", *Energies*, **8**(10), pp. 12228–12241 (2015).
27. Lima, C.H.R. and Lall, U. "Climate informed monthly streamflow forecasts for the Brazilian hydropower network using a periodic ridge regression model", *J. Hydrol.*, **380**(3-4), pp. 438–449 (2010).
28. Operacz, A., Szelag, B., and Grahl-Madsen, M. "Possibility of the modelling of electricity production from hydropower", *E3S Web Conf.*, **86** (2019).
29. Dehghani, M., Riahi-Madvar, H., Hooshyaripor, F., et al. "Prediction of hydropower generation using Grey wolf optimization adaptive neuro-fuzzy inference system", *Energies*, **12**(2), pp. 1–20 (2019).
30. Chen, J., Zeng, G.Q., Zhou, W., et al. "Wind speed forecasting using nonlinear-learning ensemble of deep learning time series prediction and extremal optimization", *Energy Convers. Manag.*, **165**(March), pp. 681–695 (2018).
31. Yu, C., Li, Y., Bao, Y., et al. "A novel framework for wind speed prediction based on recurrent neural networks and support vector machine", *Energy Convers. Manag.*, **178**(October), pp. 137–145 (2018).
32. Zhang, Z., Qin, H., Liu, Y., et al. "Long short-term memory network based on neighborhood gates for processing complex causality in wind speed prediction", *Energy Convers. Manag.*, **192**(January), pp. 37–51 (2019).
33. Liang, S., Nguyen, L., and Jin, F. "A multi-variable stacked long-short term memory network for wind speed forecasting", *Proc. - 2018 IEEE Int. Conf. Big Data, Big Data 2018*, pp. 4561–4564 (2019).
34. Wang, J., and Li, Y. "Multi-step ahead wind speed prediction based on optimal feature extraction, long short term memory neural network and error correction strategy", *Appl. Energy*, **230**(April 2018), pp. 429–443 (2018).
35. Liu, H., Mi, X., and Li, Y. "Smart multi-step deep learning model for wind speed forecasting based on variational mode decomposition, singular spectrum analysis, LSTM network and ELM", *Energy Convers. Manag.*, **159**(November 2017), pp. 54–64 (2018).
36. Balluff, S., Bendfeld, J., and Krauter, S. "Short term wind and energy prediction for offshore wind farms using neural networks", *Int. Conf. Renew. Energy Res. Appl. ICRERA*, **5**, pp. 379–382 (2015).
37. Shi, X., Lei, X., Huang, Q., et al. "Hourly day-ahead wind power prediction using the hybrid model of variational model decomposition and long short-term memory", *Energies*, **11**(11), pp. 1–20 (2018).
38. Muzaffar, S., and Afshari, A. "Short-term load forecasts using LSTM networks", *Energy Procedia*, **158**, pp. 2922–2927 (2019).
39. Arslan, N. and Sekertekin, A. "Application of long short-term memory neural network model for the reconstruction of MODIS land surface temperature images", *J. Atmos. Solar-Terrestrial Phys.*, **194**(June), p. 105100 (2019).
40. Han, S., Qiao, Y., Yan, J., et al. "Mid-to-long term wind and photovoltaic power generation prediction based on copula function and long short term memory network", *Appl. Energy*, **239**(January), pp. 181–191 (2019).
41. Zhang, J., Yan, J., Infield, D., et al. "Short-term forecasting and uncertainty analysis of wind turbine power based on long short-term memory network and Gaussian mixture model", *Appl. Energy*, **241**(October 2018), pp. 229–244 (2019).
42. Zhang, Z., Ye, L., Qin, H., et al. "Wind speed prediction method using shared weight long short-term memory network and Gaussian process regression", *Appl. Energy*, **247**(March), pp. 270–284 (2019).

43. Abyaneh, H.Z., Nia, A.M., Varkeshi, M.B., et al. "Performance evaluation of ANN and ANFIS models for estimating garlic crop evapotranspiration", *J. Irrig. Drain. Eng.*, **137**(5), pp. 280–286 (2011).

44. Jang, J.-S.R. "ANFIS: adaptive-network-based fuzzy inference system", *IEEE Trans. Syst. Man. Cybern.*, **23**(3), pp. 665–685 (1993).

45. Karakuş, O., Kuruoğlu, E.E., and Altinkaya, M.A. "One-day ahead wind speed/power prediction based on polynomial autoregressive model", *IET Renew. Power Gener.*, **11**(11), pp. 1430–1439 (2017).

46. Tabari, H., Kisi, O., Ezani, A., et al. "SVM, ANFIS, regression and climate based models for reference evapotranspiration modeling using limited climatic data in a semi-arid highland environment", *J. Hydrol.*, **444**(445), pp. 78–89 (2012).

47. Mathworks. https://ch.mathworks.com/solutions/deep-learning.html. Accessed November 30, 2020.

48. Van Houdt, G., Mosquera, C., and Nápoles, G. "A review on the long short-term memory model", *Artif. Intell. Rev.*, **53**(8), pp. 5929–5955 (2020).

49. Gers, F.A., Schraudolph, N.N., and Schmidhuber, J. "Learning precise timing with LSTM recurrent networks", *J. Mach. Learn. Res.*, **3**(1), pp. 115–143 (2003).

50. Hochreiter, S. and Schmidhuber, J. "Long short-term memory", *Neural Comput.*, **9**(8), pp. 1735–1780 (1997).

51. Ekanayake, P., Wickramasinghe, L., Jayasinghe, J.M.J.W., et al. "Regression-based prediction of power generation at samanalawewa hydropower plant in Sri Lanka using machine learning", *Math. Probl. Eng.*, **2021** (2021).

52. Jung, J., Han, H., Kim, K., et al. "Machine learning-based small hydropower potential prediction under climate change", *Energies*, **14**(12) (2021).

53. Lotfi, E., Babrzadeh, S., and Khosravi, A. "Sensitivity analysis of economic variables using neuro-fuzzy approach", *Sci. Iran.*, **27**(3D), pp. 1352–1359 (2020).

54. Turkish Electricity Transmission Corporation, https://www.teias.gov.tr/. Accessed December 4, 2020.

55. Aksoy, B. "Estimation of energy produced in hydroelectric power plant industrial automation using deep learning and hybrid machine learning techniques", *Electr. Power Components Syst.*, **49**(3), pp. 213–232 (2021).

56. Filho, A.R.G., Silva, D.F.C., de Carvalho, R.V., et al. "Forecasting of water flow in a hydroelectric power plant using LSTM recurrent neural network", *2nd Int. Conf. Electr. Commun. Comput. Eng.* (2020).

57. Ogliari, E., Nespoli, A., Mussetta, M., et al. "A hybrid method for the run-of-the-river hydroelectric power plant energy forecast: HYPE hydrological model and neural network", *Forecasting*, **2**(4), pp. 410–428 (2020).

58. Huangpeng, Q., Huang, W., and Gholinia, F. "Forecast of the hydropower generation under influence of climate change based on RCPs and developed crow search optimization algorithm", *Energy Reports*, **7**, pp. 385–397 (2021).

Biographies

Mehmet Bilgili is a faculty member at the Department of Mechanical Engineering, Cukurova University, Turkey. In 1992, he received a BSc degree at the Mechanical Engineering Department, from Cukurova University. He received MSc (2003) and PhD (2007) degrees at the Mechanical Engineering Department from Cukurova University. He has been working as a Professor of Energy at Cukurova University since 2017. He has many scientific studies on wind energy, renewable energy, heating-ventilating and air-conditioning system, and the application of artificial neural networks methods.

Sinan Keiyinci is a Research Assistant at the Department of Automotive Engineering, Cukurova University. He completed his BSc and MSc degrees in the Civil Aviation Department of Erciyes University, Kayseri and his PhD in 2021 at the University of Cukurova. He is interested in alternative energy systems.

Firat Ekinci was born in Adana, Turkey. He received the MSc and PhD degrees at the Department of Mechanical Engineering from Cukurova University, Turkey in 2001 and 2016, respectively. He has been working at Adana Alparslan Turkes Science and Technology University as an Associate Professor since 2020. His research interests include renewable energy sources, artificial neural networks, and energy systems. Dr. Ekinci has authored more than 20 technical papers published in journals and conference proceedings.